

Transfer matrix in counting problems

Roberto da Silva¹, Silvio R. Dahmen¹, J. R. Drugowich de Felício²

¹ - Instituto de Física, Universidade Federal do Rio Grande do Sul, Porto Alegre, Rio Grande do Sul, Brazil

² - Departamento de Física, Faculdade de Filosofia, Ciências e Letras de Ribeirão Preto, Universidade de São Paulo, Ribeirão Preto, São Paulo, Brazil

Abstract

The transfer matrix is a powerful technique that can be applied to statistical mechanics systems as for example in the calculus of the entropy of the ice model. One interesting way to study such systems is to map it onto a 3-color problem. In this paper, we explicitly build the transfer matrix for the 3-color problem in order to calculate the number of possible configurations for finite systems with free, periodic in one direction and toroidal boundary conditions (periodic in both directions)

1. Introduction

The transfer matrix technique in statistical physics was introduced by Kramers and Wannier in 1941 in the context of two-dimensional ferromagnetic systems [1, 2]. However its applicability extends beyond spin models [3, 4, 5, 6, 7, 8]. They are very useful not only in the description of the thermodynamics of such systems [9, 10], but can also be applied to more general settings, for example in Optics [11] and Graph theory [12]. Its foundation goes back to the roots of counting problems in statistical mechanics. If in one dimension the application of the concept in order to calculate the number of configurations is straightforward, in higher dimensions the concept has its caveats. In this paper, we wish to show how one may use the transfer matrix to study counting problems of systems in lattices considering different boundary conditions.

We can think of the problem in a more general way: we have an interacting system where the objects (spins, or colors, or other objects that we can be interested) are disposed in a two-dimensional rectangular lattice. For the sake of simplicity, let us suppose a square lattice, $L \times L$. The number of bonds between all pairs of nearest neighbor sites depends on the boundary condition of the problem. If it is free, one has $2L(L-1)$ bonds, if periodic in one of directions $L(2L-1)$, and if periodic in both directions, one has $2L^2$ bonds, as exemplified in Fig. 1 for $L=3$.

Here, we are denoting σ_j by $(\sigma_1^{(j)}, \dots, \sigma_L^{(j)})^t$ which is a particular configuration of j -th column. Now comes the most important question of this article: how to compute the number of possible configurations of the system for different boundary conditions. The answer depends on what we have at hand and how the interactions between the spins or other constituents are.

Let $T(\sigma_i, \sigma_j)$ denote the number of configurations resulted from interaction between the column σ_i with the column σ_j . T is the so-called transfer matrix of the two-dimensional system under analysis. If one has L columns, represented respectively by the vectors $\sigma_1, \sigma_2, \dots, \sigma_L$, and the interaction takes place only between nearest neighbors, the number of possible configurations is given by:

$$\Omega(L) = \sum_{\sigma_1} \sum_{\sigma_2} \dots \sum_{\sigma_L} T(\sigma_1, \sigma_2) T(\sigma_2, \sigma_3) \dots T(\sigma_{L-1}, \sigma_L) T(\sigma_L, \sigma_1) \quad (1)$$

where the sum is performed over all possible values of $\sigma_1, \dots, \sigma_L$.

This result certainly depends on how $T(\sigma_i, \sigma_j)$ was built, i.e. whether we consider free or periodic boundary conditions. If we consider free boundary conditions, that is all interactions between successive elements along the column are accounted for except between $\sigma_L^{(j)}$ and $\sigma_1^{(j)}$, we denote the transfer matrix by T_{FBC} . On the other hand, if the interaction between $\sigma_L^{(j)}$ and $\sigma_1^{(j)}$ is also included, thus we will denote the transfer matrix by T_{PBC} .

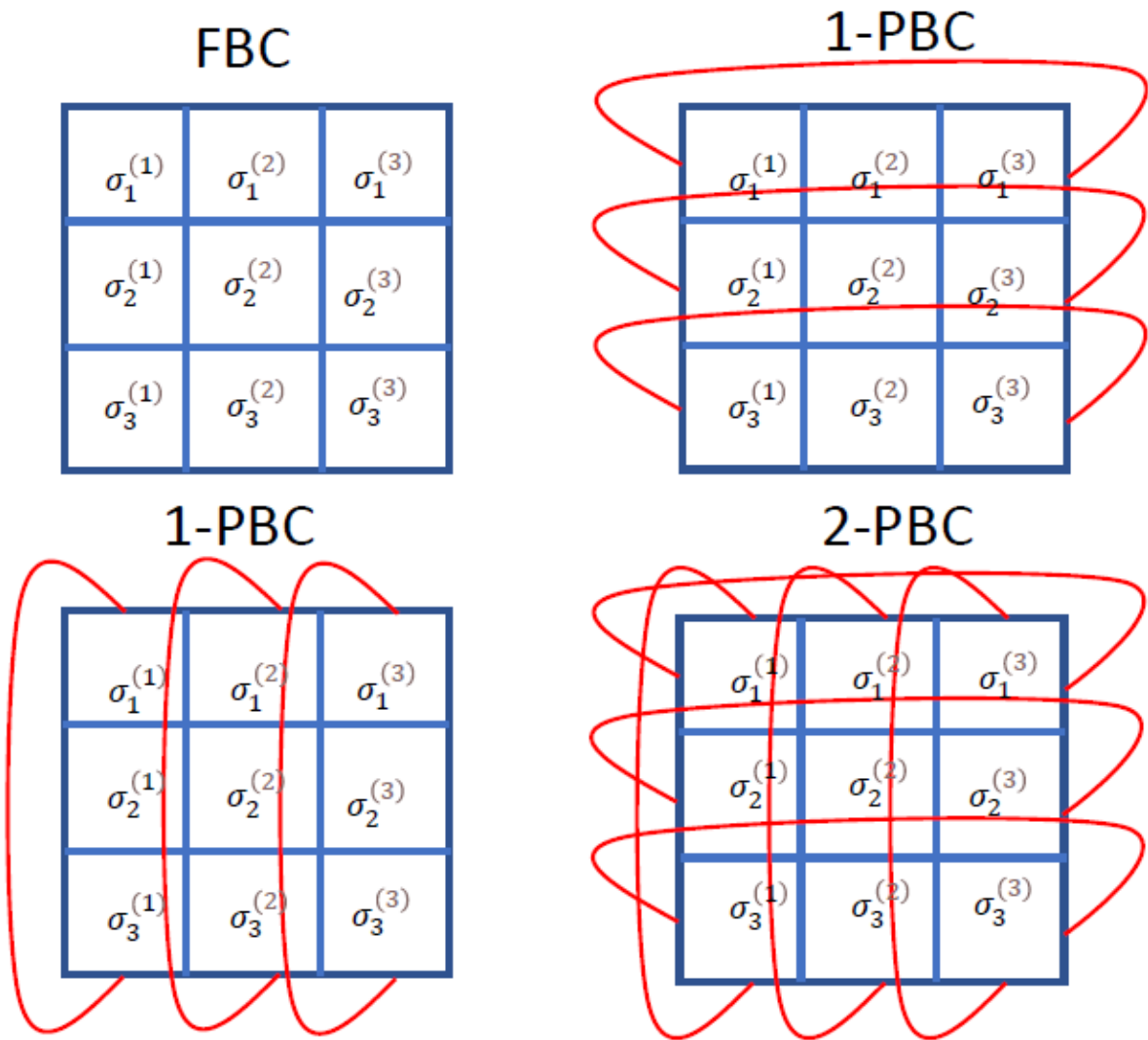


Figure 1: Different boundary conditions that can be considered when using the transfer matrix technique.

The question now is how to obtain the different cases depicted in Fig. 1 from T_{FBC} and T_{PBC} . Actually, there are only three different cases since the situations of Fig. 1 (b) and Fig. 1 (c) are symmetric. For that, we will simply use the term FBC to describe the case of Fig. 1 (a), 1-PBC will be used to describe the situations that present periodic boundary condition in only one direction: Fig 1 (b) and Fig 1 (c), and finally 2-PBC describes the situation of the Fig. 1 (d), i.e., periodic boundary conditions in both directions.

For example, from T_{FBC} we can obtain the counting Ω for FBC or 1-PBC and from T_{PBC} we can obtain Ω for 1-PBC or 2-PBC. If we want PBC in the second direction (along the rows) we simply attribute the value $T(\sigma_1, \sigma_L) = 1$.

Our first case is to calculate $\Omega_{FBC}(L)$, the number of configurations with FBC. Thus using the multiplicative principle and considering the sum over all configurations and the considerations above, one has:

$$\begin{aligned}\Omega_{FBC}(L) &= \sum_{\sigma_1} \sum_{\sigma_2} \dots \sum_{\sigma_L} T_{FBC}(\sigma_1, \sigma_2) T_{FBC}(\sigma_2, \sigma_3) \dots T_{FBC}(\sigma_{L-1}, \sigma_L) \\ &= \sum_{\sigma_1} \sum_{\sigma_L} T_{FBC}^{L-1}(\sigma_1, \sigma_2) \\ &= \text{Add}(T_{FBC}^{L-1}),\end{aligned}\tag{2}$$

where $\text{Add}(X)$ denotes the sum of all elements of the matrix X .

Naturally, $C_{1-PBC}(L)$ can be also calculated using T_{FBC} . In this case $T_{FBC}(\sigma_L, \sigma_1)$ is not set to 1 in the expression. From this we obtain the important cyclical property of the trace:

$$\begin{aligned}\Omega_{1-PBC}(L) &= \sum_{\sigma_1} \sum_{\sigma_2} \dots \sum_{\sigma_L} T_{FBC}(\sigma_1, \sigma_2) T_{FBC}(\sigma_2, \sigma_3) \dots T_{FBC}(\sigma_{L-1}, \sigma_L) T_{FBC}(\sigma_L, \sigma_1) \\ &= \text{Tr}(T_{FBC}^L)\end{aligned}\tag{3}$$

However, if we already have periodic boundary conditions in one direction in (T_{PBC}) we can also obtain $C_{1-PBC}(L)$. However in this case we take $T_{PBC}(\sigma_1, \sigma_L) = 1$:

$$\begin{aligned}\Omega_{1-PBC}(L) &= \sum_{\sigma_1} \sum_{\sigma_2} \dots \sum_{\sigma_L} T_{PBC}(\sigma_1, \sigma_2) T_{PBC}(\sigma_2, \sigma_3) \dots T_{PBC}(\sigma_{L-1}, \sigma_L) \\ &= \sum_{\sigma_1} \sum_{\sigma_L} T_{PBC}^{L-1}(\sigma_1, \sigma_2) \\ &= \text{Add}(T_{PBC}^{L-1}).\end{aligned}\tag{4}$$

With this we can calculate $C_{1-PBC}(L)$ in two different ways: using T_{FBC} (Eq. 3) or T_{PBC} (Eq. 4). Finally to obtain $C_{2-PBC}(L)$ one has only one possibility: one starts with T_{PBC} and completes it to obtain the PBC in the other direction:

$$\begin{aligned}\Omega_{2-PBC}(L) &= \sum_{\sigma_1} \sum_{\sigma_2} \dots \sum_{\sigma_L} T_{PBC}(\sigma_1, \sigma_2) T_{PBC}(\sigma_2, \sigma_3) \dots T_{PBC}(\sigma_{L-1}, \sigma_L) T_{PBC}(\sigma_L, \sigma_1) \\ &= \text{Tr}(T_{FBC}^L)\end{aligned}\tag{5}$$

In a recent and more didactic work [13], we showed how to implicitly use the transfer matrix method to obtain the entropy of the two-dimensional ice-type model mapping the problem onto the three-color problem. However two important points were not considered in our approach:

1. The method did not explicitly explore the properties of the matrices, something which is done in detail in the present work;
2. Moreover, we present the results for the case of toroidal boundary conditions, extending Creswick's method [14] that considers periodic boundary conditions in one direction only.

We obtain $C(L)$ for different boundary conditions only by switching between equations 2, 3, 4, and 5. We also show that using periodic boundary conditions in both directions yields better estimates than previously obtained in [13]. The paper is organized as follows: for the sake of completeness we present in the next section the ice-type model, a two-dimensional structure proposed to explain the residual entropy of ice at $T = 0$ [15]. Finally, we show how this problem can be mapped in the three-color problem.

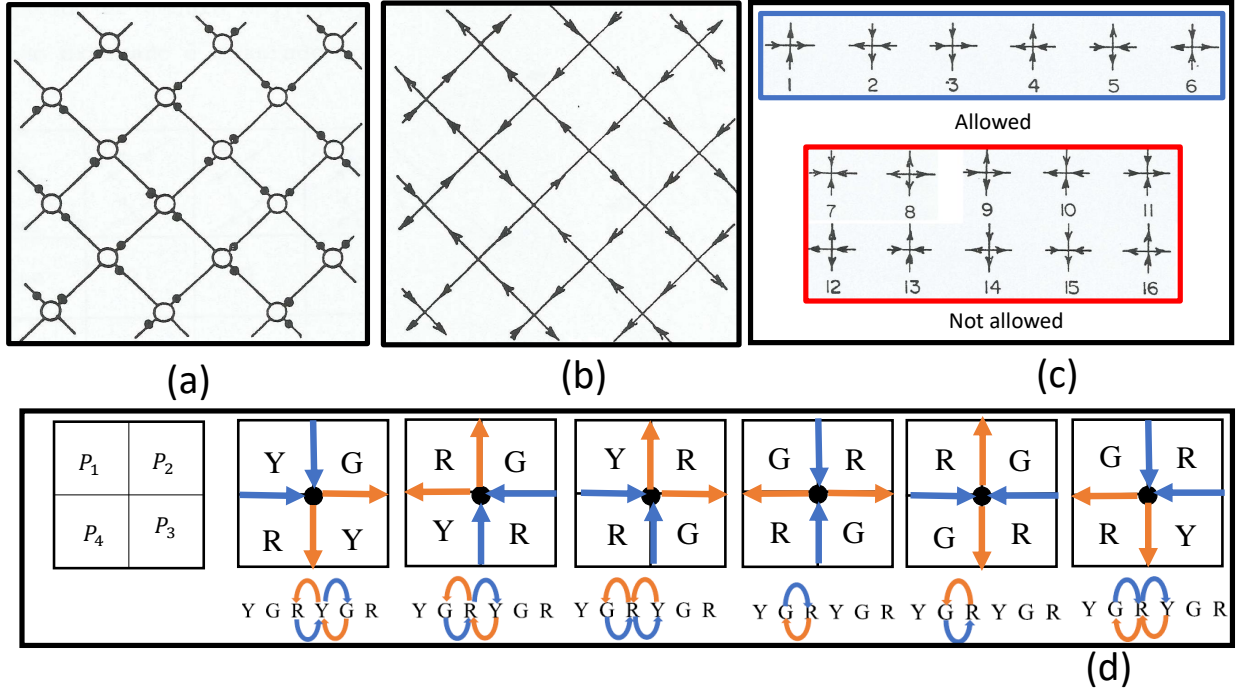


Figure 2: (a) The two-dimensional ice model. White circles represent oxygen atoms while black ones stand for hydrogen; (b) Representation of (a) using arrows; (c) the six different configurations of arrows allowed in the ice-model and the prohibited ones; (d) mapping of the six-vertex model onto the three-color problem.

We then present the simplest cases ($L = 1, 2$, and 3) and we explicitly evaluate $\Omega(L)$ for each case. In what follows, we present the results considering an efficient computer routine for cases with $L > 3$ and we estimate the entropy of the system extrapolating $L \rightarrow \infty$ for every boundary condition considered. Finally, we present some considerations and conclusions suggesting that our approach can be extended to other counting problems in Statistical Physics.

2. The ice-type model and its mapping onto the three-color problem

Ice has a tetrahedral structure with oxygen atoms occupying the vertices. Each oxygen is linked by hydrogen bonds to four other oxygen atoms. This means that if we wish to consider a two-dimensional version of this model it has to preserve the fundamental characteristics of the real structure which is the fact that each oxygen atom has four neighbours. Since each water molecule has only two hydrogen atoms, in the real structure two of these hydrogen atoms must be in the nearest equilibrium position and the two other at the larger distance. In Fig. 2 (a) we show a two dimensional representation of this ice-type model. White circles represent O atoms, while black ones represent hydrogen ones.

Since each hydrogen atom can be in two distinct positions, Pauling [15] introduced an arrow to indicate whether it is near to (incoming arrow) or far from (outcoming arrow) an oxygen. The percentage of H_3O^+ and OH^- ions are taken as zero which means that each O atom (site in the lattice) must necessarily have 2 and only 2 hydrogen atoms next to it (two incoming and two outcoming arrows from a vertex). Fig. 2 (b) is the same as Fig. 2 (a) represented as arrows. From the 16 possible types of vertices, only six satisfy the so-called ‘ice rules’ (Fig. 2 (c)), introduced by Bernal and Fowler in 1933 [16] and improved by Linus Pauling [15].

On the other hand, it is very interesting to recast this problem using the language of map coloring. For that, we attribute three colors, yellow (Y), green (G), and red (R) to countries in a world represented by a two dimensional lattice. For example a 2×2 -world with 4 countries is represented in Fig. 2 (d), where P_1, P_2, P_3 , and P_4 denote countries. Let us call a *proper* coloring of the map one where countries with a common border are colored differently

while in the opposite case they could have the same color. For example P_1 must be different from P_2 and P_4 , but it could have the same color as P_3 . In the same Fig. 2 (d) we can observe 6 particular examples of proper colorings of a 2×2 -world with a maximal of three colors, resulting in the six possible different arrow configurations of the six-vertex model.

We shall use a cyclical convention for the colours: Y follows G , G follows R , and R follows Y ($YGRYGRYGR\dots$). Every time we rotate the map clockwise with respect to a perpendicular axis going through the common vertex (black dot) of each 2×2 -map inserted in the whole $L \times L$ -map. Starting for example from P_1 , if we change from yellow to green (green to red, red to yellow) the arrow (depicted blue) in the boundary will be directed to the common point, while the changing from red to green (green to yellow, yellow to red) is represented by an orange arrow leaving the common point. This applies both for the horizontal as well as the vertical boundaries. This common point that resembles the position of oxygen atoms will always have two arrows in and two arrows out. Fig. 2 (d) shows the six possible configurations of arrows and colors on a map. Let us consider the first color configuration in that same figure. We start in P_1 with Y and P_1 with G . Going clockwise there is a blue vertical arrow pointing to the vertex. From P_2 to P_3 , one has G to Y in the counter-clockwise direction, and thus there is an orange horizontal arrow off the vertex. From P_3 to P_4 there is an orange vertical arrow off the vertex, and from P_4 to P_1 there is a blue horizontal incoming arrow. Other colorings (there are another 12 different colorings in addition to the six shown in the example) in this mapping only lead to one of the possible arrow configurations depicted in this same figure.

In fact, each configuration of arrows corresponds to three possible colorings in fig. 2 (d), since there are three possible colors for P_1 to start with. Thus we can write

$$\Omega_{\text{colours}}(L) = 3\Omega_{\text{six-vertex}}(L). \quad (6)$$

Denoting $L^2 = N$, we define $\Omega_{\text{six-vertex}}(L) = W^N$ and thus the entropy of the ice-type model is given by:

$$S = k_B \ln \Omega_{\text{six-vertex}} = N k_B \ln W \quad (7)$$

The idea now is to estimate W by calculating $\Omega_{\text{colours}}(L)$ through an extrapolation via the transfer matrix. But before doing that, we can better understand how to estimate $\Omega_{\text{colours}}(L)$ if we look at some simple cases explicitly.

3. Some explicit examples: Pedagogical aspects

Let us show how the method works by constructing and calculating T_{FBC} and T_{PBC} for the simplest non trivial cases $L = 2$ and $L = 3$ and after. For $L = 2$, note that $T_{FBC} = T_{PBC}$. We thus use simply T for the transfer matrix since we compose it by crossing states $|\varphi\rangle = |C_1 C_2\rangle$. For a proper coloring, C_1 and C_2 must be different.

With 3 colors, of a total of 9 possible configurations only $n_{\text{max}} = 6$ different states are allowed. For example $|RG\rangle$ is a possible state while $|RR\rangle$ is not. Thus for two states $|\varphi_1\rangle = |C_1^{(1)} C_2^{(1)}\rangle$ and $|\varphi_2\rangle = |C_1^{(2)} C_2^{(2)}\rangle$, the scalar product $\langle\varphi_1|\varphi_2\rangle = \langle\varphi_2|\varphi_1\rangle$ is defined by:

$$\langle\varphi_1|\varphi_2\rangle = \begin{cases} 1 & \text{if } C_1^{(1)} \neq C_1^{(2)} \text{ and } C_2^{(1)} \neq C_2^{(2)} \\ 0 & \text{otherwise} \end{cases} \quad (8)$$

We can thus explicitly write $T(L = 2)$ as:

$$T = \begin{pmatrix} & |YR\rangle & |RY\rangle & |GR\rangle & |RG\rangle & |YG\rangle & |GY\rangle \\ \langle YR| & 0 & 1 & 0 & 1 & 0 & 1 \\ \langle RY| & 1 & 0 & 1 & 0 & 1 & 0 \\ \langle GR| & 0 & 1 & 0 & 1 & 1 & 0 \\ \langle RG| & 1 & 0 & 1 & 0 & 0 & 1 \\ \langle YG| & 0 & 1 & 1 & 0 & 0 & 1 \\ \langle GY| & 1 & 0 & 0 & 1 & 1 & 0 \end{pmatrix} \quad (9)$$

In this particular case $C_{FBC} = C_{1-PBC} = C_{2-PBC}$, and therefore, $Tr(T^2) = Add(T) = 18$. Is it easy to understand this result: in a world with 4 countries ($L = 2$) and 3 colors we can paint P_1 and P_3 with same or with different colors. If they have the same color, there are 3 colors to choose and P_2 and P_4 , which of course must be different from the previous ones. The number of ways is thus:

$$f_{=}(3) = \underbrace{3}_{P_1 \text{ and } P_3} \times \underbrace{2}_{P_2} \times \underbrace{2}_{P_4} = 12 \quad (10)$$

The other possibility is to put different colors in P_1 and P_3 . In this case P_2 and P_4 , which must differ from the former, can only be painted in one color. Thus:

$$f_{\neq}(3) = \underbrace{3 \times 2}_{P_1 \text{ and } P_3} \times \underbrace{1}_{P_2} \times \underbrace{1}_{P_4} = 6 \quad (11)$$

Consequently the number of different colorings of a 2×2 -world is

$$f(3) = f_{=}(3) + f_{\neq}(3) = 18, \quad (12)$$

which is exactly the number we found via matrix operations.

One may also observe that such result can be checked in two other ways, if our prescriptions are correct: a) computing $T^2(L = 2)$ and directly taking the trace of T^2 , or, b) calculating the eigenvalues of T , and using the fact that $Tr(T^n) = \sum_{i=1}^{n_{\max}} \lambda_i^n$. Calculating T^2 explicitly, one has

$$T^2 = \begin{pmatrix} 3 & 0 & 2 & 1 & 2 & 1 \\ 0 & 3 & 1 & 2 & 1 & 2 \\ 2 & 1 & 3 & 0 & 1 & 2 \\ 1 & 2 & 0 & 3 & 2 & 1 \\ 2 & 1 & 1 & 2 & 3 & 0 \\ 1 & 2 & 2 & 1 & 0 & 3 \end{pmatrix} \quad (13)$$

One may check that $Tr(T^2) = 6 \times 3 = 18$, which matches with our previous results. Calculating the eigenvalues of T one has: $\lambda_1 = \lambda_2 = 0$, $\lambda_3 = 3$, $\lambda_4 = 1$, and $\lambda_5 = \lambda_6 = -2$, and $0^2 + 0^2 + 3^2 + 1^2 + (-2)^2 + (-2)^2 = 18$ as expect. The case $L = 2$ is simple and more investment is necessary to understand the method.

To better understand the procedure and check the conjectures, we must study the case $L = 3$ where we have $T_{FBC} \neq T_{PBC}$. Defining now states $|\varphi\rangle = |C_1 C_2 C_3\rangle$, we have a total of 27 candidate states. Here we can consider two possibilities: C_1 must be different from C_2 (PBC) or not (FBC). In the case of T_{FBC} , we have $n_{\max} = 12$ different possible states $|C_1 C_2 C_3\rangle$ since the color C_1 can be equal to C_3 , and the only restriction is in the situations $C_1 \neq C_2$ and $C_2 \neq C_3$. Thus we have:

$$T_{FBC} = \begin{pmatrix} & |GYR\rangle & |RYG\rangle & |RYR\rangle & |GYG\rangle & |GRY\rangle & |YRG\rangle & |GRG\rangle & |YRY\rangle & |YGR\rangle & |RGY\rangle & |YGY\rangle & |RGR\rangle \\ \langle GYR| & 0 & 0 & 0 & 0 & 0 & 1 & 0 & 1 & 0 & 1 & 1 & 0 \\ \langle RYG| & 0 & 0 & 0 & 0 & 1 & 0 & 0 & 1 & 1 & 0 & 1 & 0 \\ \langle RYR| & 0 & 0 & 0 & 0 & 1 & 1 & 1 & 1 & 0 & 0 & 1 & 0 \\ \langle GYG| & 0 & 0 & 0 & 0 & 0 & 0 & 0 & 1 & 1 & 1 & 1 & 1 \\ \langle GRY| & 0 & 1 & 1 & 0 & 0 & 0 & 0 & 0 & 1 & 1 & 0 & 1 \\ \langle YRG| & 1 & 0 & 1 & 0 & 0 & 0 & 0 & 0 & 0 & 1 & 0 & 1 \\ \langle GRG| & 0 & 0 & 1 & 0 & 0 & 0 & 0 & 0 & 1 & 1 & 1 & 1 \\ \langle YRY| & 1 & 1 & 1 & 1 & 0 & 0 & 0 & 0 & 0 & 0 & 0 & 1 \\ \langle YGR| & 0 & 1 & 0 & 1 & 1 & 0 & 1 & 0 & 0 & 0 & 0 & 0 \\ \langle RGY| & 1 & 0 & 0 & 1 & 1 & 1 & 1 & 0 & 0 & 0 & 0 & 0 \\ \langle YGY| & 1 & 1 & 1 & 1 & 0 & 0 & 1 & 0 & 0 & 0 & 0 & 0 \\ \langle RGR| & 0 & 0 & 0 & 1 & 1 & 1 & 1 & 1 & 0 & 0 & 0 & 0 \end{pmatrix} \quad (14)$$

Calculating T_{FBC}^2 , one has:

$$T_{FBC}^2 = \begin{pmatrix} 4 & 2 & 3 & 3 & 1 & 1 & 2 & 0 & 0 & 1 & 0 & 2 \\ 2 & 4 & 3 & 3 & 1 & 0 & 2 & 0 & 1 & 1 & 0 & 2 \\ 3 & 3 & 5 & 2 & 0 & 0 & 1 & 0 & 2 & 3 & 1 & 4 \\ 3 & 3 & 2 & 5 & 3 & 2 & 4 & 1 & 0 & 0 & 0 & 1 \\ 1 & 1 & 0 & 3 & 5 & 3 & 4 & 3 & 1 & 0 & 2 & 0 \\ 1 & 0 & 0 & 2 & 3 & 4 & 3 & 3 & 0 & 1 & 2 & 0 \\ 2 & 2 & 1 & 4 & 4 & 3 & 5 & 2 & 0 & 0 & 1 & 0 \\ 0 & 0 & 0 & 1 & 3 & 3 & 2 & 5 & 2 & 2 & 4 & 1 \\ 0 & 1 & 2 & 0 & 1 & 0 & 0 & 2 & 4 & 3 & 3 & 3 \\ 1 & 1 & 3 & 0 & 0 & 1 & 0 & 2 & 3 & 5 & 3 & 4 \\ 0 & 0 & 1 & 0 & 2 & 2 & 1 & 4 & 3 & 3 & 5 & 2 \\ 2 & 2 & 4 & 1 & 0 & 0 & 0 & 1 & 3 & 4 & 2 & 5 \end{pmatrix} \quad (15)$$

So if one calculates $Add(T_{FBC}^2)$, it yields the number of configurations of a 3×3 -map with free boundary conditions in both directions. This results in 246. This can be checked by computing all possibilities with a simple algorithm (see for example [13]). We will check this when we find T_{PBC} . However if one wants to obtain the result with periodic boundary conditions in one direction, the only possibility is to take $Tr(T_{FBC}^3)$. Evaluating T_{FBC}^3 explicitly, one has:

$$T_{FBC}^3 = \begin{pmatrix} 2 & 1 & 4 & 3 & 8 & 10 & 6 & 14 & 8 & 11 & 14 & 7 \\ 1 & 2 & 3 & 4 & 11 & 8 & 7 & 14 & 10 & 8 & 14 & 6 \\ 4 & 3 & 2 & 10 & 17 & 15 & 15 & 17 & 6 & 6 & 14 & 3 \\ 3 & 4 & 10 & 2 & 6 & 6 & 3 & 14 & 15 & 17 & 17 & 15 \\ 8 & 11 & 17 & 6 & 2 & 1 & 3 & 5 & 13 & 16 & 9 & 18 \\ 10 & 8 & 15 & 6 & 1 & 2 & 3 & 3 & 8 & 13 & 6 & 15 \\ 6 & 7 & 15 & 3 & 3 & 3 & 2 & 9 & 15 & 18 & 14 & 18 \\ 14 & 14 & 17 & 14 & 5 & 3 & 9 & 2 & 6 & 9 & 3 & 14 \\ 8 & 10 & 6 & 15 & 13 & 8 & 15 & 6 & 2 & 1 & 3 & 3 \\ 11 & 8 & 6 & 17 & 16 & 13 & 18 & 9 & 1 & 2 & 5 & 3 \\ 14 & 14 & 14 & 17 & 9 & 6 & 14 & 3 & 3 & 5 & 2 & 9 \\ 7 & 6 & 3 & 15 & 18 & 15 & 18 & 14 & 3 & 3 & 9 & 2 \end{pmatrix} \quad (16)$$

Summing the diagonal elements gives 24 ways. The eigenvalues of T_{FBC} yield the same result: numerically, up to 15 significant figures, they are: $\lambda_1 = 4.561552812808830$, $\lambda_2 = -3.414213562373095$, and $\lambda_3 = -3.414213562373093$. The last two values are probably the same eigenvalue with multiplicity 2, since there is agreement in 14 digits. One has further $\lambda_4 = 1.999999999999998$, which probably is 2, $\lambda_5 = 1.000000000000001$, $\lambda_6 = \lambda_7 = 1.000000000000000$. Finally $\lambda_8 = \lambda_9 = -1.000000000000000$, $\lambda_{10} = -5.857864376269052 \times 10^{-1}$, $\lambda_{11} = -5.857864376269045 \times 10^{-1}$ (probably, again, multiple eigenvalues), and $\lambda_{12} = 4.384471871911689 \times 10^{-1}$.

From these results follow $\sum_{i=1}^{12} \lambda_i^3 = 24.000000000000035$, which says that we have 24 ways to paint a world with 9 countries (3×3 -lattice) with periodic boundary condition in only one direction (within the numerical precision stated above).

Now let us obtain T_{PBC} . This matrix can be obtained from T_{FBC} by excluding the columns and rows whose states have $C_1 = C_3$, which reduces the problem to a matrix of dimension $n_{\max} = 6$.

$$T_{PBC} = \begin{pmatrix} & |GYR\rangle & |RYG\rangle & |GRY\rangle & |YRG\rangle & |YGR\rangle & |RGY\rangle \\ \langle GYR| & 0 & 0 & 0 & 1 & 0 & 1 \\ \langle RYG| & 0 & 0 & 1 & 0 & 1 & 0 \\ \langle GRY| & 0 & 1 & 0 & 0 & 1 & 1 \\ \langle YRG| & 1 & 0 & 0 & 0 & 0 & 1 \\ \langle YGR| & 0 & 1 & 1 & 0 & 0 & 0 \\ \langle RGY| & 1 & 0 & 1 & 1 & 0 & 0 \end{pmatrix} \quad (17)$$

First, we can test if we can obtain the result for periodic boundary conditions in one direction. We need to calculate $Add(T_{PBC}^2)$:

$$T_{PBC}^2 = \begin{pmatrix} 2 & 0 & 1 & 1 & 0 & 1 \\ 0 & 2 & 1 & 0 & 1 & 1 \\ 1 & 1 & 3 & 1 & 1 & 0 \\ 1 & 0 & 1 & 2 & 0 & 1 \\ 0 & 1 & 1 & 0 & 2 & 1 \\ 1 & 1 & 0 & 1 & 1 & 3 \end{pmatrix} \quad (18)$$

from which we obtain $Add(T_{PBC}^2) = 24$ exactly as we expect. But, what if one wants the number of possibilities

with periodic boundary conditions in both directions? The eigenvalues of T_{PBC} can in this case be calculated exactly (numerically if needed) and their values are $\lambda_1 = \sqrt{2} + 1, \lambda_2 = 1 - \sqrt{2}, \lambda_3 = \sqrt{3}, \lambda_4 = -\sqrt{3}, \lambda_5 = \lambda_6 = -1$. Therefore $\sum_{i=1}^6 \lambda_i^3 = (\sqrt{2} + 1)^3 - (\sqrt{2} - 1)^3 - 2 = 12$.

In case one does not want to calculate eigenvalues, one may again take the power T_{PBC}^3 and the trace:

$$T_{PBC}^3 = \begin{pmatrix} 2 & 1 & 1 & 3 & 1 & 4 \\ 1 & 2 & 4 & 1 & 3 & 1 \\ 1 & 4 & 2 & 1 & 4 & 5 \\ 3 & 1 & 1 & 2 & 1 & 4 \\ 1 & 3 & 4 & 1 & 2 & 1 \\ 4 & 1 & 5 & 4 & 1 & 2 \end{pmatrix} \quad (19)$$

which yields $Tr(T_{PBC}^3) = 12$, thus corroborating the previous result. The problem, in this particular case, can be understood as a 3×3 -*sudoku*. We can count these 12 possibilities that respect PBC in both directions. The simplest way to perform such counting by hand is to fix the first color in the first country and to analyze all possibilities for each choice. For each choice there are only 4 possibilities, since we can choose the first country in 3 different ways, which yields a total of 12 as represented in Eq. 20.

R <i>G</i> <i>Y</i>	R <i>G</i> <i>Y</i>	R <i>Y</i> <i>G</i>	R <i>Y</i> <i>G</i>
<i>G</i> <i>Y</i> <i>R</i>	<i>Y</i> <i>R</i> <i>G</i>	<i>G</i> <i>R</i> <i>Y</i>	<i>Y</i> <i>G</i> <i>R</i>
<i>Y</i> <i>R</i> <i>G</i>	<i>G</i> <i>Y</i> <i>R</i>	<i>Y</i> <i>G</i> <i>R</i>	<i>G</i> <i>R</i> <i>Y</i>
Y <i>R</i> <i>G</i>	Y <i>R</i> <i>G</i>	Y <i>G</i> <i>R</i>	Y <i>G</i> <i>R</i>
<i>R</i> <i>G</i> <i>Y</i>	<i>G</i> <i>Y</i> <i>R</i>	<i>R</i> <i>Y</i> <i>G</i>	<i>G</i> <i>R</i> <i>Y</i>
<i>G</i> <i>Y</i> <i>R</i>	<i>R</i> <i>G</i> <i>Y</i>	<i>G</i> <i>R</i> <i>Y</i>	<i>R</i> <i>Y</i> <i>G</i>
G <i>Y</i> <i>R</i>	G <i>Y</i> <i>R</i>	G <i>R</i> <i>Y</i>	G <i>R</i> <i>Y</i>
<i>R</i> <i>G</i> <i>Y</i>	<i>Y</i> <i>R</i> <i>G</i>	<i>Y</i> <i>G</i> <i>R</i>	<i>R</i> <i>Y</i> <i>G</i>
<i>Y</i> <i>R</i> <i>G</i>	<i>R</i> <i>G</i> <i>Y</i>	<i>R</i> <i>Y</i> <i>G</i>	<i>Y</i> <i>G</i> <i>R</i>

(20)

Since we analyzed the simplest cases by making explicit the matrices and showing how the method works, we are prepared to numerically study the problem and perform an extrapolation $N \rightarrow \infty$.

4. Numerical results and finite-size effects via an efficient computational method.

Our task begins by building the matrices T_{FBC} and T_{PBC} , and find n_{\max} (the number of states) as a function of L . But as we have seen previously, this is not a difficult task: for example n_{\max} for FBC is exactly the number of ways of painting a unidimensional world with L countries without periodic boundary conditions with three colors. This is equivalent to paint a strip since P_1 is not a neighbor of P_L (Fig. 3-a). On the other hand, for PBC P_1 is a neighbor of P_L , and this amounts to painting the pizza-chart as shown in Fig. 3-b.

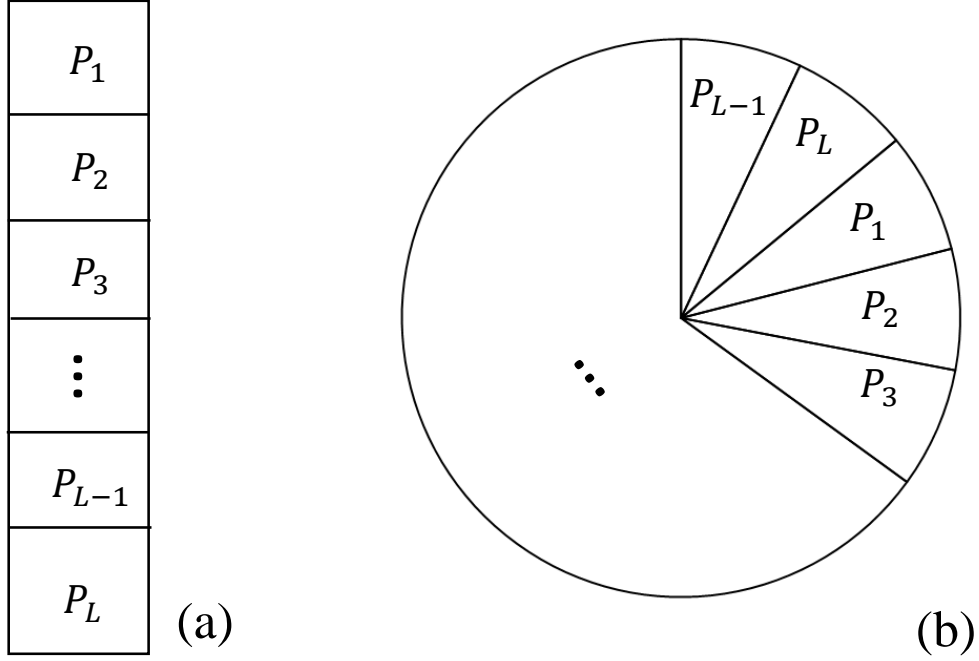


Figure 3: Determination of the number of allowed states (n_{\max}) for obtaining T_{FBC} and T_{PBC} .

In the first case we have 3 possibilities for P_1 , but since P_1 cannot have the same color as P_2 , there are 2 possibilities for the latter. P_2 cannot share a color with P_3 , which gives also 2 possibilities for P_3 and so on. With L countries we have $n_{\max}^{FBC}(L) = 3 \times 2^{L-1}$. However the second situation is more complicate. Let us denote this number by $n_{\max}^{PBC}(L)$. We can think for example the case where P_1 and P_3 have the same color or different ones. In the first case, we have a situation where two sectors merge into one and the same sector. Thus, for each coloring of the pizza-chart with $L-2$ sectors composed by the sector originated from the fusion of P_1 with P_3 and all the remaining $L-3$ sectors (except P_2), one has 2 ways to paint the sector P_2 which can have neither the same color of P_1 nor that of P_3 . On the other hand if P_1 necessarily has a color different from P_3 , so there is only one way to color P_2 . In this case we have to paint the pizza-chart with $L-1$ sectors (all except P_2). Both situations are independent and we can write a simple recurrence relation: $n_{\max}^{PBC}(L) = 2 \times n_{\max}^{PBC}(L-2) + n_{\max}^{PBC}(L-1)$. Its solution leads to $n_{\max}^{PBC}(L) = 2^L + 2(-1)^L$. (This can be checked by direct substitution)

Our task now is to build T_{FBC} and T_{PBC} . We know the number of all states, and each state is built in the following way:

$$|\varphi\rangle_{FBC} = |C_1 C_2 \dots C_L | \delta_{C_i, C_{i+1}} = 0, \text{ for all } i = 1 \dots L-1 \rangle \quad (21)$$

or

$$|\varphi\rangle_{PBC} = |C_1 C_2 \dots C_L | \delta_{C_i, C_{i+1}} = 0, \text{ for all } i = 1 \dots L, \text{ and } C_{L+1} = C_1 \rangle. \quad (22)$$

To each of the allowed states $|\varphi^{(j)}\rangle$, $j = 1, \dots, n_{\max}$ a number $n(j) = \sum_{l=0}^{L-1} C_l^{(j)} 4^l$ is associated, with $C_i^{(j)} = 0, 1, 2$ where we made the association $Y \rightarrow 0$, $G \rightarrow 1$, and $R \rightarrow 2$. So to determine the matrix $T(j, j') = \langle \varphi^{(j)} | \varphi^{(j')} \rangle$, we can use two interesting operators: the first one is the *exclusive-OR* operator (IEOR(i_1, i_2) in Fortran) which returns the bitwise Boolean exclusive-OR of integer i_1 and i_2 , that is if bits are the same, the result is 0. If not, it returns the result 1. For example if $i_1 = (1001)_2$ and $i_2 = (1111)_2$, one has IEOR(i_1, i_2) = $(0110)_2$. The second is an operator that returns a logical true if the bit at p in q is set, and the counting of the bits starts at 0. In FORTRAN, the operator has a syntax: BTEST(q, p). For example the IEOR($n(j), n(j')$) makes the exclusive OR operation “bit by bit” of the

L	$n_{\max}^{(FBC)}$	$Add(T_{FBC}^{L-1})$	$Tr(T_{FBC}^L)$	$\sum_{i=1}^{n_{\max}} (\lambda_{FBC}^{(i)})^L$	$\lambda_{FBC}^{(\max)}$
2	6	18	18	18	3
3	12	246	24	24.0000000000000040	4.561552812808830
4	24	7812	4626	4625.99999999995000	6.971960768397091
5	48	580986	38880	38879.99999999990000	10.682885121208430
6	96	$1.01596896 \cdot 10^8$	$3.7284186 \cdot 10^7$	$3.7284186000000060 \cdot 10^7$	16.392041198957880
7	192	$4.1869995708 \cdot 10^{10}$	$1.886476032 \cdot 10^9$	$1.886476032000011 \cdot 10^9$	25.174078531617520
8	384	$4.0724629633188 \cdot 10^{13}$	$9.527634436194 \cdot 10^{12}$	$9.52763443619383 \cdot 10^{12}$	38.683160866531850
9	768	$9.357497524902707 \cdot 10^{16}$	$2.825260002442752 \cdot 10^{15}$	$2.825260002442852 \cdot 10^{15}$	59.465107914794780
10	1536	$5.082795214936645 \cdot 10^{20}$	$7.704801938642910 \cdot 10^{19}$	$7.704801938642726 \cdot 10^{19}$	91.437962270582820

Table 1: Results from T_{FBC}

two binaries $n(j)$ and $n(j')$.

The result gives a binary sequence of $2L$ bits. Taking bits by pairs, i.e., the first and the second, third and the fourth, and so on, if one or more of these pairs is 00, it implies that some neighboring countries share the same color. This can be performed by executing the operation $BTEST(IEOR(n(j), n(j')), k)$ to check if bit k is 0 or 1. Thus we can write that:

$$T(j, j') = \begin{cases} 1 & \text{if } \prod_{\substack{k=1 \\ k \text{ odd}}}^{2L-1} [BTEST(IEOR(n(j), n(j')), k) + BTEST(IEOR(n(j), n(j')), k+1)] \neq 0 \\ 0 & \text{otherwise} \end{cases} \quad (23)$$

Let us consider a particular case with $L = 3$. For example $|\varphi^{(j)}\rangle = |C_1^{(j)} C_2^{(j)} C_3^{(j)}\rangle = |101\rangle = 1 \times 4^0 + 0 \times 4^1 + 1 \times 4^2 = 17 = 1 \times 2^0 + 0 \times 2^1 + 0 \times 2^2 + 0 \times 2^3 + 1 \times 2^4 + 0 \times 2^5 = (100010)_2$ and $|\varphi^{(j')}\rangle = |C_1^{(j')} C_2^{(j')} C_3^{(j')}\rangle = |120\rangle = 1 \times 4^0 + 2 \times 4^1 + 0 \times 4^2 = 9 = 1 \times 2^0 + 0 \times 2^1 + 0 \times 2^2 + 1 \times 2^3 + 0 \times 2^4 + 0 \times 2^5 = (100100)_2$. In this binary representation we can consider that 00 corresponds to Y , 01 corresponds to G , and finally 10 corresponds to R . So the result $IEOR(n(j), n(j')) = IEOR(17, 9)$ can explicitly calculated as:

17	1	0	0	0	1	0
9	1	0	0	1	0	0
IEOR(17,9)	0	0	0	1	1	0

(24)

and one has that $BTEST(IEOR(n(j), n(j')), 1) = 0$ and $BTEST(IEOR(n(j), n(j')), 1) = 0$ and thus $T(j, j') = 0$ according Eq. 23.

Since we understand how to computationally build the matrices, we can show our main results. We performed numerical experiments computing values using both methods for a double-check: by directly calculating and then by computing the eigenvalues.

Tables 1 and 2 show the results for T_{FBC} and T_{PBC} respectively. We can observe as expected that the fourth (or fifty) column in 1 leads to same result represented in the third column of 2. The fifth column in Table 1 is just used as a cross-check of the fourth column, exactly as in Table 2.

But what does these results mean? To see that we can estimate from the results obtained from the tables the quantity:

$$W = \left(\frac{1}{3}\Omega\right)^{1/N} \quad (25)$$

which essentially is the exponential of the entropy per particle divided by the Boltzmann constant. We will now perform an extrapolation $\lim_{N \rightarrow \infty} W = W_\infty$. In the next subsection, we will present an ingenious method to do such an extrapolation by the use of successive polynomial fits. Finally in subsection 4.2 we apply a more precise technique

L	$n_{\max}^{(PBC)}$	$Add(T_{PBC}^{L-1})$	$Tr(T_{PBC}^L)$	$\sum_{i=1}^{n_{\max}} (\lambda_{PBC}^{(i)})^L$	$\lambda_{PBC}^{(\max)}$
2	6	18	18	18	3
3	6	24	12	11.999999999999999	2.000000000000000
4	18	4626	2970	2970.000000000000000	6.372281323269014
5	30	38880	7560	7559.999999999950000	5.999999999999998
6	66	$3.7284186 \cdot 10^7$	$1.64484 \cdot 10^7$	$1.644839999999986 \cdot 10^7$	14.506431494048050
7	126	$1.886476032 \cdot 10^9$	$1.9900062 \cdot 10^8$	$1.990006199999976 \cdot 10^8$	15.783341876392290
8	258	$9.527634436194 \cdot 10^{12}$	$2.901094068042 \cdot 10^{12}$	$2.901094068041933 \cdot 10^{12}$	33.676786957721970
9	510	$2.825260002442752 \cdot 10^{15}$	$1.825277062836360 \cdot 10^{14}$	$1.825277062836212 \cdot 10^{14}$	39.650566012033250
10	1026	$7.704801938642287 \cdot 10^{19}$	$1.617804974008648 \cdot 10^{19}$	$1.617804974008630 \cdot 10^{19}$	78.818864591827550

Table 2: Results from T_{PBC}

Boundary conditions	$n = 1$	$n = 2$	$n = 3$	$n = 4$
FBC	1.644(16)	1.6122(81)	1.5907(37)	1.572(32)
1 - PBC (even branch)	1.616(13)	1.5868(46)	1.5733(22)	1.566(26)
2 - PBC (even branch)	1.5360(16)	1.539749(26)	1.539675(22)	1.5395980(27)
1 - PBC (odd branch)	1.466(54)	1.5733(47)	1.5608(18)	1.555(15)
2 - PBC (odd branch)	1.387(64)	1.5143(81)	1.5358(11)	1.53947(13)

Table 3: Values of W for the different cases: FBC, 1-PBC, and 2-PBC. We also separate the results in even and odd branch to perform better extrapolations the corresponding uncertainties for $n = 1, 2$, and 3 are due to uncertainty in the intercept after the polynomial extrapolation. The estimates for $n = 4$ exactly appears with error bars since we used the difference between the extrapolated value and the exact value $(4/3)^{(3/2)}$. It is important to mention that for this case the uncertainty in the intercept cannot be estimated since the number of points is exactly the number parameters in the interpolation

due to Bulirsch and Stoer [17] and later applied to Statistical Mechanics [18].

4.1. Polynomial Extrapolation

First let us analyze the extrapolation $W \times N^{-1}$ for *FBC* which can be seen in Fig. 4. Different polynomial fits were performed to obtain an extrapolation $\lim_{N \rightarrow \infty} W = W_{\infty}$. Line 2 of table 3 shows that the higher the polynomial degree n the better the extrapolated value W_{∞} , since the exact value for W_{∞} is $W_{lieb} = 1.5396007...$ (see ref. [5]). For FBC the results are not so good since the best result is $W_{\infty} = 1.572 \pm 0.032$ (we are keeping the number of digits for trustworthiness). It is important to observe that we are using

the simplest case for elaborating the plots, that is $L = 1$ and $\Omega = 3$. In which case it is trivial to see that it does not depend on the boundary conditions. Thus it is important to go beyond that, by studying the cases 1-PBC and 2-PBC.

We generated plots of $W \times 1/N$ for 1-PBC, as depicted in Fig. 5 (a) and for 2-PBC, as depicted in Fig. 5 (b). It is interesting to observe that in the case of PBC, an alternating convergence is observed. Just for the sake of comparison, in Fig. 5 (c) we observe that the highest eigenvalue of T_{PBC} increases and oscillates while T_{FBC} does not present this oscillation between odd and even values of L , showing that the highest eigenvalue seems to reflect the behavior observed in $W \times 1/N$ in Figs. 4 and 5 (a) and (b).

Once we observed this oscillatory behavior in the convergence for PBC between odd and even values of L , we separate the extrapolation in two branches: odd and even. Figs. 6 (a), (b), (c), and (d) show the polynomial fits for each case considered/studied.

The rows in table 3 show the extrapolated value for each case. We can observe that for periodic boundary conditions in both directions leads to a match with the exact result until the fourth digit. Our results with transfer-matrix leads to results better than we alternatively found in [13], however it is necessary to separate the extrapolation in different branches. Such extrapolation can be obtained by using a method really precise when compared with successive polynomial extrapolations with higher degrees. In the following, we present the BST method by applying in our model which gives really good estimates and mainly it does not require a separation of the data in odd and even branches.

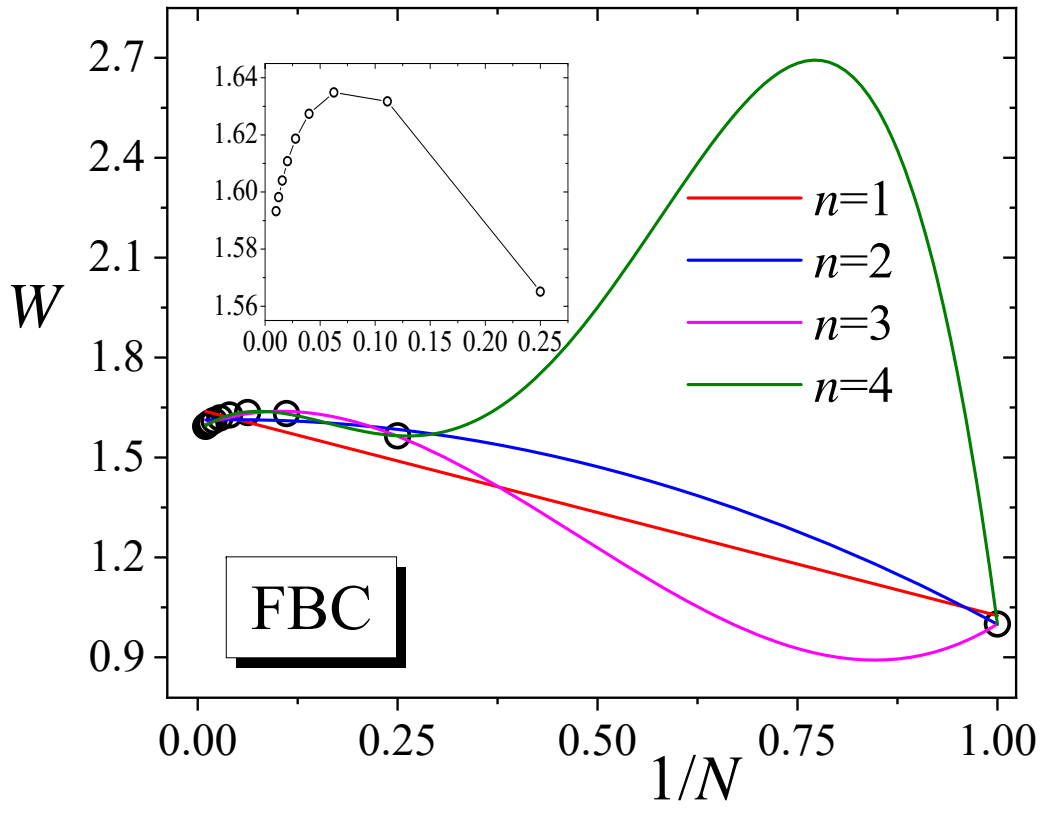


Figure 4: $W \times 1/N$ for FBC. We perform fits with polynomials of degree 1, 2, 3, and 4.

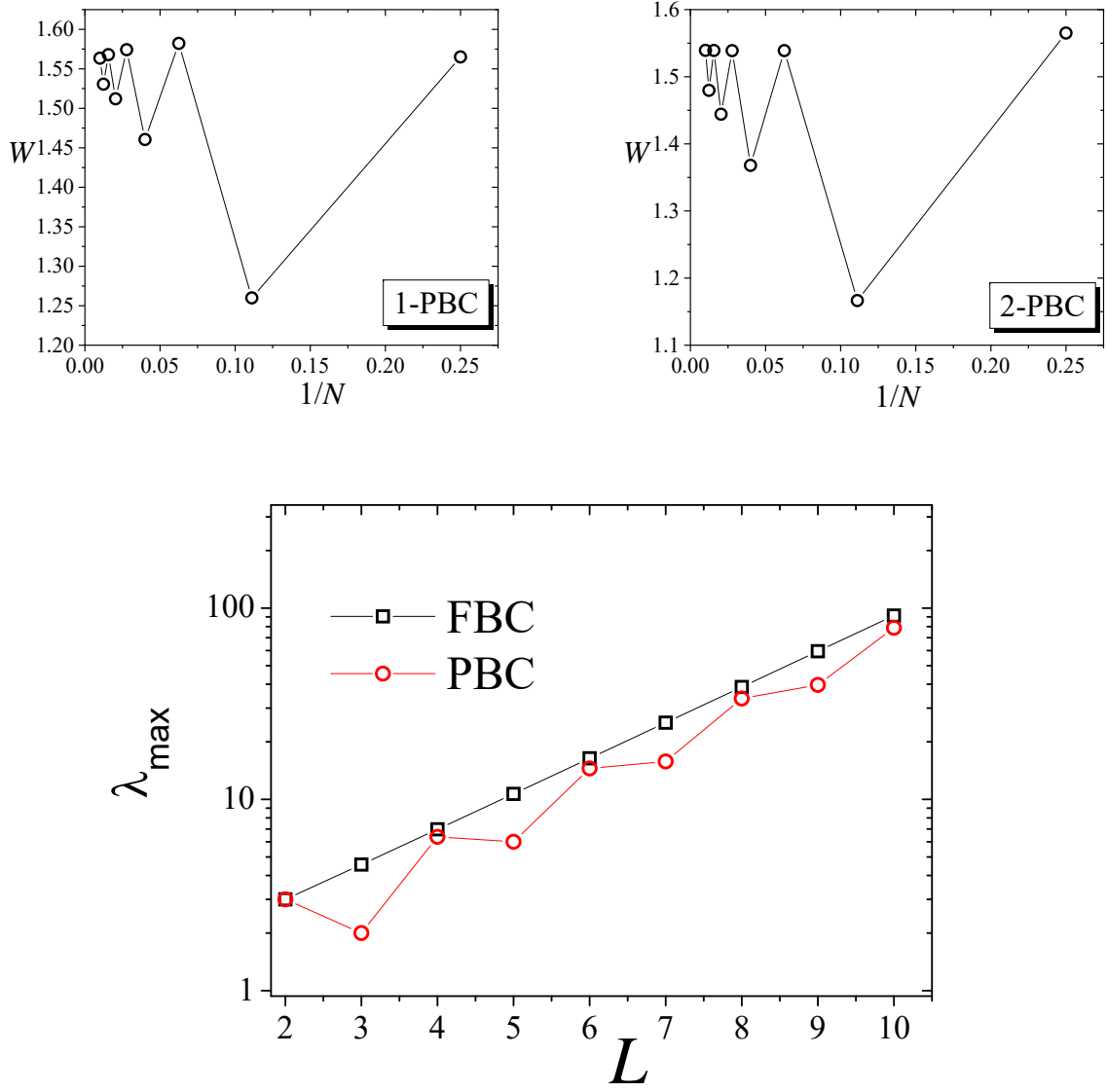


Figure 5: $W \times 1/N$ for 1-PBC (a) and 2-PBC (b). It is interesting to observe that in the case of the PBC, an alternating convergence is observed. In the plot (c), we observe that the highest eigenvalue of T_{PBC} grows up oscillating while T_{FBC} does not present this oscillation between odd and even L values.

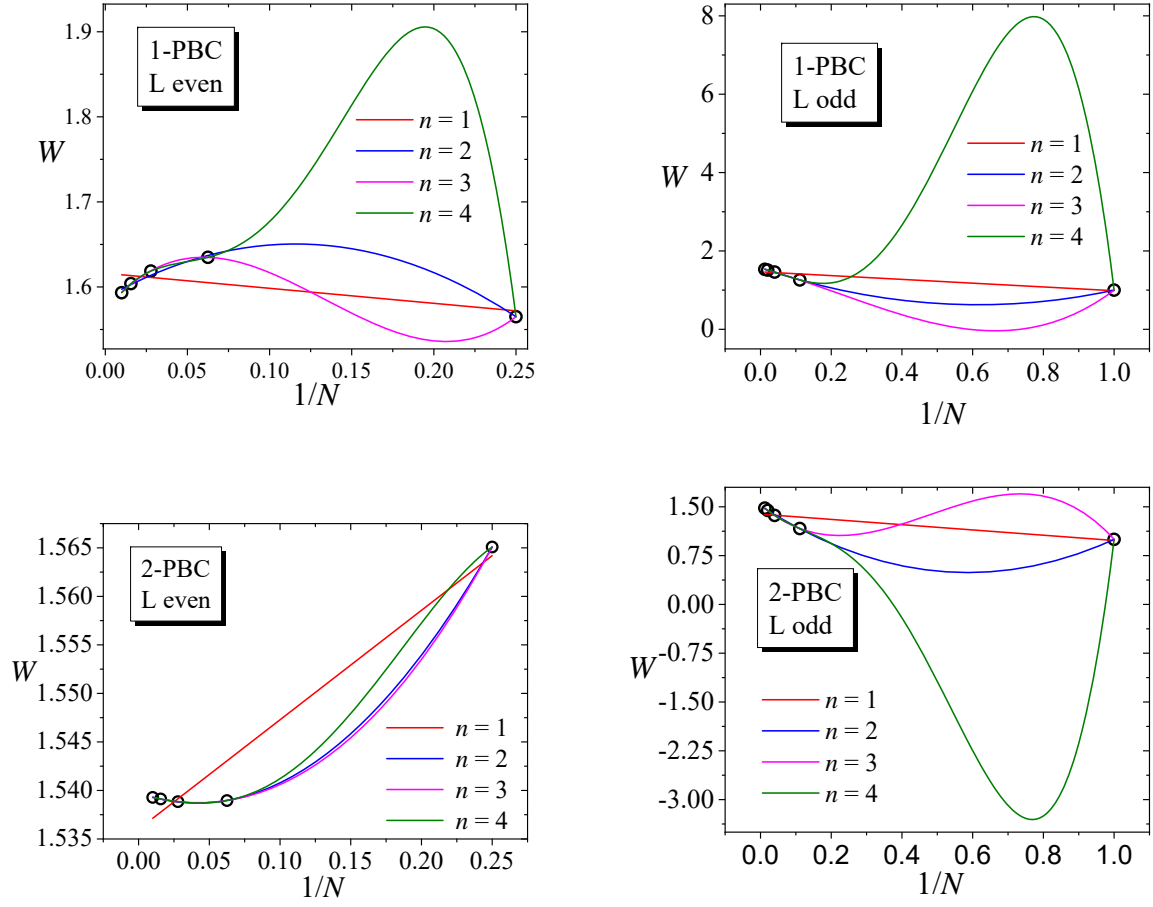


Figure 6: Extrapolation of $W \times 1/N$ for 1-PBC and 2-PBC. (a) Even branch of 1-PBC, (b) Odd branch of 1-PBC, (c) Even branch of 2-PBC, and (d) Odd branch of 2-PBC

4.2. Refined extrapolation: The Bulirsch-Stoer (BST) method

By assuming that W is given by the expansion:

$$W = W_\infty + a_1 h_L + a_2 h_L^2 + \dots$$

where $h_L = \frac{1}{L^2}$, with $L = 1, 2, 3, 4, \dots$, one get $W \rightarrow W_\infty$ in the limit $L \rightarrow \infty$. The BST method considers a sequence of extrapolants [18], which in our case can be given by:

$$\begin{aligned} W_{n,m} &= W_{n+1,m-1} + \frac{(W_{n+1,m-1} - W_{n,m-1})}{\left[\left(\frac{h_{n+1}}{h_{n+m+1}} \right)^\omega \left(1 - \frac{(W_{n+1,m-1} - W_{n,m-1})}{(W_{n+1,m-1} - W_{n,m-2})} \right) - 1 \right]} \\ &= W_{n+1,m-1} + \frac{(W_{n+1,m-1} - W_{n,m-1})}{\left[\left(\frac{n+m+1}{n+1} \right)^{2\omega} \left(1 - \frac{(W_{n+1,m-1} - W_{n,m-1})}{(W_{n+1,m-1} - W_{n,m-2})} \right) - 1 \right]} \end{aligned} \quad (26)$$

where ω is a free parameter.

Considering that one has the values of W for $L = 1, 2, \dots, L_{\max}$, represented by $W_{0,0}, W_{1,0}, W_{2,0}, \dots, W_{L_{\max}-1,0}$, from Eq. 26 one obtains the subsequent values. However such extrapolation is based on a binary tree, according to the table of extrapolants:

$$\begin{array}{ccccccc} & & W_{0,0} & & & & \\ & & & W_{0,1} & & & \\ W_{1,0} & & & & W_{0,2} & & \\ & & & W_{1,1} & & \searrow & \\ W_{2,0} & & \vdots & & \vdots & & \dots W_{0,L_{\max}-1} \\ & & \vdots & & \vdots & & \\ & & W_{L_{\max}-3,1} & & & \nearrow & \\ W_{L_{\max}-2,0} & & & W_{L_{\max}-3,2} & & & \\ & & W_{L_{\max}-2,1} & & & & \\ W_{L_{\max}-1,0} & & & & & & \end{array} \quad (27)$$

where with $W_{0,0}$ and $W_{1,0}$, one obtains $W_{0,1}$, with $W_{1,0}$ and $W_{2,0}$, one obtains $W_{1,1}$, and so successively. The same rule is used to obtain the subsequent generations until one obtains $W_{0,L-1}$ which is the best approximant to W_∞ , the root of the binary tree. This is computationally performed by considering that for each $m = 1, \dots, L_{\max} - 1$, n goes from 0 to $L - 1 - m$.

In order to determine the suitable ω_{opt} we can take ω ranging from an ω_{\min} until ω_{\max} , with a resolution $\Delta\omega$, to find the best $W_{0,L_{\max}-1} = W_{opt}$ such that $\xi = |W_{0,L_{\max}-1} - W_\infty|$ be minimized since we know $W_\infty = (4/3)^{3/2}$.

Fig. 7 shows a plot of ξ versus ω considering $\omega_{\min} = 0$ and $\omega_{\max} = 8$, with $\Delta\omega = 8 \cdot 10^{-4}$. For FBC (Fig. 7 (a)) and 2-PBC (Fig. 7 (c)) we found respectively $\omega_{opt} = 0.5096$ and $\omega_{opt} = 3.0664$, whose determine respectively $W_{opt}(\text{FBC}) = 1.539602 \pm 0.000002$ and $W_{opt}(\text{2-PBC}) = 1.53960073 \pm 0.00000001$. By illustration, it is interesting to show the sequence of iterations in the binary tree as represented by Eq. 27. For FBC one has the BST approximants represented in a binary tree in Table 4.

Similarly for the 2-PBC case, the sequence of iterations is represented in table 5.

We considered the 1-PBC as a separate case, since its convergence was more delicate and thus $L = 10$ was not enough to obtain good estimates via BST method. Based on this point, we extended our initial values considering $L = 15$. In this case we really obtained good results as shown in Fig.7 (b), which gives $\omega_{opt}(\text{1-PBC}) = 2.1996$, resulting in $W_{opt}(\text{1-PBC}) = 1.53960063 \pm 0.00000008$ which supplies a much better estimate when compared with the linear fit performed in [13].

We summarized our main results from BST in Table 6.

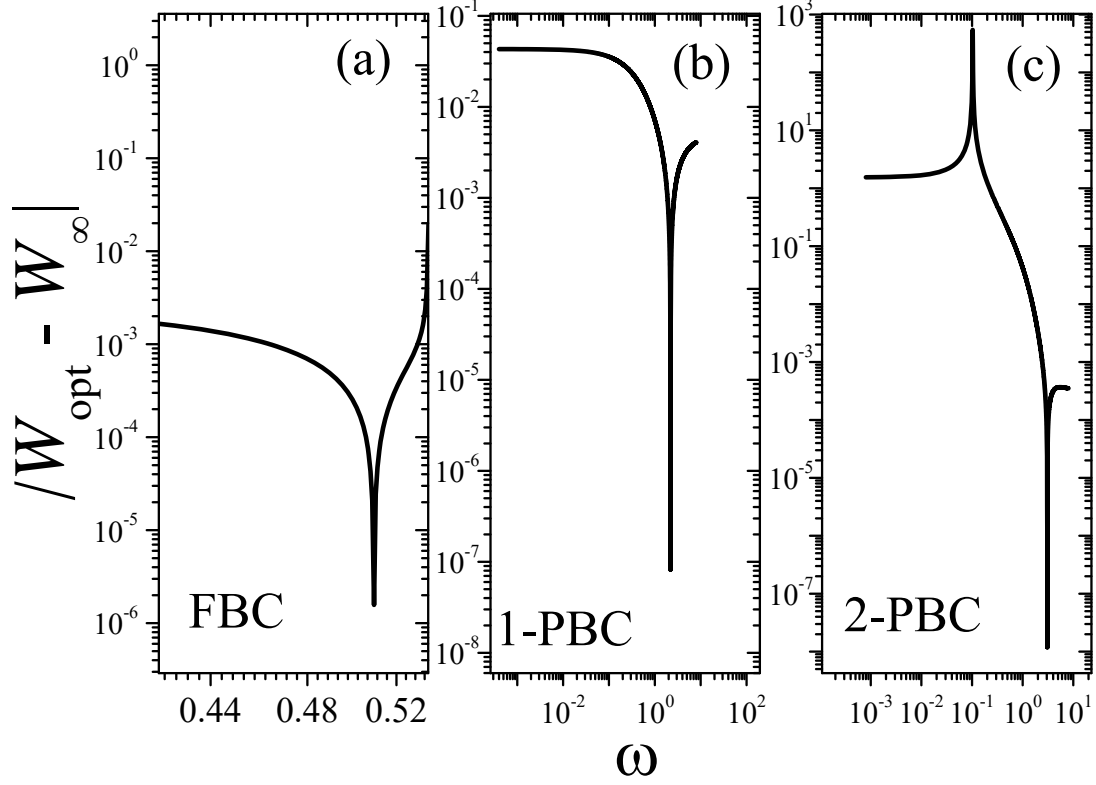


Figure 7: $\xi = |W_{opt} - W_{\infty}|$ as function of ω for FBC, 1-PBC, and 2-PBC

$W_{n,m}$	$m=0$	$m=1$	$m=2$	$m=3$	$m=4$	$m=5$	$m=6$	$m=7$	$m=8$	$m=9$
	1.000000000									
		3.480583082								
	1.565084577		1.715219692							
		1.779807114		1.550250173						
	1.631721258		1.638260759		1.537231234					
		1.644097339		1.540048426		1.538396031				
	1.634848714		1.630430852		1.538278167		1.539911992			
		1.598650546		1.538863512		1.538867985		1.539577074		
	1.627353072		1.740465533		1.538869734		1.539605491		1.539654610	
		1.577487753		1.538867110		1.538862496		1.539674735		1.539602290
	1.618676186		1.449058272		1.539171458		1.539658715		1.539616720	
		1.565882904		1.539021038		1.542237835		1.539517684		
	1.610780478		1.514524921		1.539345304		1.539560599			
		1.558840107		1.539166123		1.539683697				
	1.603980184		1.527719176		1.539434047					
		1.554254763		1.539273370						
	1.598196268		1.532769420							
		1.551109328								
	1.593271613									

Table 4: BST approximants for FBC with $L = 1, 2, \dots, 10$

$W_{n,m}$	$m = 0$	$m = 1$	$m = 2$	$m = 3$	$m = 4$	$m = 5$	$m = 6$	$m = 7$	$m = 8$	$m = 9$
	1.000000000									
		1.577975700								
	1.565084580		1.156646890							
		1.140183112		1.5448184389						
	1.166529040		1.542890160		1.343729852					
		1.647705037		1.3426505965		1.540748058				
	1.538959531		1.344749629		1.540138974		1.424988740			
		1.317901102		1.5646689105		1.424844904		1.539855817		
	1.367905267		1.538874475		1.425146964		1.539590605		1.465328620	
		1.638264392		1.4216357309		1.549157927		1.465299279		1.539600730
	1.538843701		1.429591658		1.539035457		1.465363450		1.539462458	
		1.389882824		1.5681790646		1.464633278		1.544169675		
	1.444199558		1.539029999		1.466430923		1.539171586			
		1.623256319		1.4588169435		1.552046417				
	1.539120096		1.470888365		1.539170223					
		1.427676251		1.5392230356						
	1.479705887		1.539223036							
		1.610686315								
	1.539281498									

Table 5: BST approximants for 2-PBC with $L = 1, 2, \dots, 10$

Lattice	ω_{opt}	W_{opt}
FBC	0.5096	1.539602(2)
1-PBC	2.1996	1.53960063(8)
2-PBC	3.0664	1.53960073(1)

Table 6: Final results from BST approximants

4.3. Brief comments about the numerical efforts

Our method considers the use of explicit matrices. Basically, the main point of this paper is the extension for periodic boundary conditions in both directions which necessarily demands at least $O(n_{\max}^3) = O(8^L)$ in any of the alternatives: taking powers of $n_{\max} \times n_{\max}$ matrices or simply calculating the set of eigenvalues of a single matrix $n_{\max} \times n_{\max}$. Operations to prepare the states and build the matrices are relatively faster: $O(4^L)$. In this case, the complexity is better represented by $O(8^L)$. It is computationally “expensive” since the exponent is linear in L , but the exponential dependence can be a nuisance for larger lattices.

Our intention was to show the strength of the method even when not considering large lattices. For example, a simple and interesting extrapolation method as BST works since our task is to deal with 8^L and not simply L . For example, using a processor Intel(R) Core(TM) i7-8565U CPU @ 1.80GHz-1.99 GHz with IMSL Numerical Libraries, for $L = 10$ one needs a few seconds while for $L = 12$ something around 2 minutes. This is fine for such sizes but one has to be careful: if one considers a not so large lattice size $L = 15$, one estimates a processing time around $t \approx \frac{8^{15}}{8^{12}} \times 2 \text{ min} = 2^{10} \text{ min}$, something near $t \approx 17$ hours which is still feasible but it starts to become “indigestible”

Without periodic boundary conditions in both directions, one can use an implicit method where one does not need to explicitly build the matrix (see [13]). This method is highly efficient but it only works (to the best of our knowledge) for free and periodic boundary conditions in one direction.

5. Conclusions

This work extends the numerical transfer matrix method proposed by Creswick [14] to contemplate the case of toroidal boundary conditions. The problem we deal with is the three-color one, which in turn is equivalent to the six-vertex model proposed by Pauling to explain the residual entropy of ice at $T = 0$. Our results (see table 6) agree very well with the exact result obtained by Lieb [4, 5] for square lattices $W_{lieb} = (4/3)^{3/2} \approx 1.5396007$ by solving exactly the six-vertex model, or by Baxter [6] when mapping the problem in a hard-square lattice gas, or even by

Biggs [19] when obtaining the chromatic polynomial for a finite toroidal square lattice graph exactly for three colors. No wonder all results are obtained in the thermodynamic limit and 3 colors is also very important since the number of ways to properly paint a square lattice graph with x colors, $\phi(x)$, satisfies the inequality in the thermodynamic limit [19]:

$$\frac{1}{2}(x-2+\sqrt{x^2-4x+8}) \geq \phi(x) \geq \frac{x^2-3x+3}{x-1}$$

and for $x = 3$, the both sides of this inequality assume the same value: $\phi(3) = (4/3)^{3/2} = W_{lieb}$. We differently worked with finite systems and with a subsequent extrapolation which leads to this same value, suggesting that our method could be extended for other models in statistical mechanics, where the thermodynamic limit is not known.

Finally, we also show how to obtain the results for periodic boundary conditions in only one direction from a matrix constructed with free boundary conditions and we also show how to obtain toroidal boundary conditions from a matrix previously constructed with periodic boundary conditions in one direction, which shows the flexibility of our approach. It is important to mention that our result for W is essentially the same for all boundary conditions and the uncertainties in table 6 show the numerical precision that such approaches may have.

Acknowledgments

R. da Silva thanks CNPq for financial support under grant numbers 311236/2018-9, and 424052/2018-0. The authors would like to thank the anonymous referee for suggesting the use of the BST method to perform our extrapolations. The authors also thank the Prof. P. Nightingale for kindly sending us the reprints of his manuscript [9].

References

- [1] H. A. Kramers, G. H. Wannier, Phys. Rev., **60**, 252–262 (1941)
- [2] H. A. Kramers, G. H. Wannier, Phys. Rev., **60**, 263–276 (1941)
- [3] E. A. DiMarzio, F. H. Stillinger Jr., J. Chem. Phys. **40**, 1577–1581 (1964)
- [4] E. H. Lieb, Phys. Rev. Lett. **18**, 692 (1967)
- [5] E. H. Lieb, Phys. Rev. **162**, 162 (1967)
- [6] R. J. Baxter J. Math. Phys. **11** 3116 (1970)
- [7] N. E. Pegg J. Phys. A **15** L549 (1982)
- [8] V.B. Teif, Nucleic Acids Res. **35**, e80 (2007)
- [9] M. P. Nightingale, Proc. Koninklijke Nederlandse Akademie van Wetenschappen B **82**, 235 (1979)
- [10] M. T. Batchelor, J. Australian Math. Soc. B **28** (1987) 462–475
- [11] C. C. Katsidis, D. I. Siapkas Appl. Opt. **41**, 3978–3987 (2002)
- [12] A. Engström, F. Kohl, Adv. Math., **330**, 1–37 (2018)
- [13] R. da Silva, O. Nakao, J. R. Drugowich de Felício, Eur. J. Phys. **42**, 025101 (2021)
- [14] R. J. Creswick, Phys. Rev. E **52**, R5735 (1995)
- [15] L. Pauling, J. Am. Chem. Soc. **57**, 2680 (1935)
- [16] J.D. Bernal, R. H. Fowler, J. Chem. Phys. **1**, 515 (1933)
- [17] R. Bulirsch, J. Stoer, Numer. Math. **6**, 413 (1964)
- [18] M. Henkel, G. Schutz, J. Phys. A **21**, 2617–2633 (1988)
- [19] N. Biggs Bull. Lond. Math. Soc. **9**, 54 (1977)